Journal of Radioanalytical and Nuclear Chemistry (2018) 318:1805–1819
https://doi.org/10.1007/s10967-018-6043-6

Sediment chronology and historical evolution of heavy metal contamination in terms of pollution index in Turkish coast, north Aegean Sea

I. Sert[1]

Received: 9 February 2018 / Published online: 28 July 2018

Abstract
The present study investigated two cores and fifteen surficial sediment samples in terms of chronology and pollution levels. Lead-210 (polonium-210) activity concentrations were measured through alpha spectrometry in Northern Turkish Aegean Sea. Sediment dating was conducted using lead-210 (CRS, CIC) mathematical models. Residence time of the ^{210}Pb was calculated to improve the precision of the dating there. Average residence time of the ^{210}Pb was 2.4 years and average sedimentation rate 0.237 ± 0.011 cm year^{-1} in the sea. Sedimentation rates along the cores exhibit irregular increases and decreases at the stations of Ayvalik Offshore and Bakircay River Mouth. Metal concentrations were assessed by means of pollution indexes (EF, CF, PLI, Igeo) and Lead-isotope ratios (^{206}Pb/^{207}Pb). According the Pollution Load Index, both Ayvalik offshore and Bakircay River Mouth have shown a starting level pollution from past to until recently. In terms of Geo-accumulation Index, both stations have Ca and Hg pollutions and the stations have had the "unpolluted to moderately polluted" pollution degree since 1995.

Keywords Sedimentation rate · Residence time of the ^{210}Pb · PLI · Igeo · lead isotopes

Introduction

The Aegean Sea lies in the northeastern Mediterranean, between Ionian Sea and the Levantine Sea. It is bound by the Greek mainland to the north and west, the Turkish coast to the east and the Island of the Cretan Arc to the south as well as its connection with the Marmara and Black Seas through the straits of Dardanelles and Bosphorus [1]. It has a surface area of about 1.8×10^{11} m^2, a volume of 8.5×10^{13} m^3 and a mean depth of 450 m [2]. Numerous investigations were performed there but the literature on the sediment chronology and evaluation of the element concentration in terms of its origin in Turkish coast of north Aegean Sea is not proportional to the number of investigations which are using nuclear methods. For instance, hydrothermalism of the Aegean Sea was described [3, 4] and origin and distribution of the terrigenous component of the unconsolidated surface sediment of the Aegean floor investigated [5]. Venting fluids are known to be highly enriched in natural radionuclides including ^{210}Po and its grandparent ^{210}Pb and Ca, Al are derived from biogenic debris in hydrothermal areas [6]. In addition, variations in grain size, carbonate content, sand mineralogy of surficial bottom deposits from transition in the Aegean-Çanakkale-Marmara were examined [7]. It is useful knowledge in terms of sorption capacity of radionuclide in sediment and Al, Ni originate from terrigenous supply. Microseismicity of the Milos Island, Greece was investigated to correlate the recorded earthquake signals with venting periodicity and time compositional variability of suspended particle matter in submarine of Milos Bay was studied to better understand role of episodic events [8, 9], microseismicity directly affects the Mn concentration. Distribution and possible sources of metals in the surface sediment of the Gulf of Saros were studied and impact of urban discharges on the levels of metallic contaminants also determined in Mytilene harbor and adjacent coastal

Electronic supplementary material The online version of this article (https://doi.org/10.1007/s10967-018-6043-6) contains supplementary material, which is available to authorized users.

✉ I. Sert
ilker.sert@ege.edu.tr; ilkersert@hotmail.com

[1] Institute of Nuclear Sciences, Ege University, 35100 Bornova, Izmir, Turkey

area [10, 11]. It is possible to enhance the related samples but it could be enough to give only one sample in different categories. Concerning sediment chronology and natural radioactivity, the cases is that natural radioactivity is widespread in the earth environment and exists in various seafood, marine organisms and geological formations such as soil, rocks, plants, sand, water and air.

In terms of natural and anthropogenic radioactivity, impact of shallow water hydrothermal inputs on the biogeochemical cycling of ^{210}Po and ^{210}Pb was assessed in the coastal marine environment and effects of late quaternary climatic and sea-level changes on sedimentation and paleo bathymetry off the Büyük Menderes River delta in Aegean Sea investigated [12, 13]. Natural and anthropogenic radionuclide levels and some heavy metals were determined in the sea sediments and total alpha and beta activity concentrations of sea water were measured in Aegean Sea [14]. One has determined recent chronology by lead-210 dating models, metal concentrations and hydrothermal impacts on sedimentation in Gülbahçe Bay [15].

The primary aim of the study is to determine the sediment dating of north Aegean Sea via lead-210 models, the second clarify the sedimentation pattern of the region, the third evaluate the pollution degree of study area the last investigate the relation between sedimentation pattern and accumulation of metal concentrations. To achieve the above, sediment chronology was obtained using Constant Rate of Supply and Constant Initial Concentrations mathematical models on the ground that there were profile distributions of ^{210}Pb activities along the cores. Residence time of ^{210}Pb was calculated to clarify the sediment dating and sedimentation pattern of the region. Four pollution index (Enrichment Factor, Anthropogenic Factor, Pollution Load Index, Geo-accumulation Index) were employed to evaluate the pollution degree and evaluation was supported in terms of lead isotopes (^{206}Pb/^{207}Pb ratio). Correlations between the metal concentrations were used to identify the source of the metals. Distribution of metal concentrations and sedimentation patterns were investigated to indicate the potential relationships between them.

Material and method

The present research obtained fifteen surficial sediment samples and two sediment cores cruise of the R/V Piri Reis, of the Institute of Marine Sciences and Technology Dokuz Eylül University, using a Van Veen grab sampler and box corer from the north Aegean Sea in 2014 (Fig. 1). Locations of the stations were from 39°18′6.00″N, 26°37′0.00″E to 38°26′15.33″N, 27°6′6.52″E In North–south direction, water depths varied between 16 and 132 m, sediment core lengths were 39 and 30 cm and surficial sediments represented the upper 5 cm of the sea floor.

Polonium-210 and lead-210 radionuclides

There are two stages in preparation of samples for analysis. The first is physical preparation which consists of the following steps. The cores were removed from the PVC pipes and cut in intervals of 1 cm. Before sediment samples were oven dried, wet weights of the samples were noted, then ground and passed through a 63 μm mesh to obtain homogenization. The second which consists of the chemical steps is used for the radiochemical analysis. One completely dissolved 1 g sample and standardized 0.1 Bq mL^{-1} amount of ^{209}Po (half-life: 103 years) internal tracer (National Institute of Standards and Technology, $<$ 500 Bq in 7% hydrochloric acid) in HF:HNO_3 (1:1) and HCl in Teflon beaker. With the addition of the ascorbic acid to the 0.5 M HCl solution polonium was spontaneously plated onto copper discs in it. Ascorbic acid was used to reduce ferrum ions [16]. To measure ^{210}Po concentrations of 5.30 MeV alpha particles emission to stem from ^{210}Po, ^{210}Po-accumulated cupper discs were counted by alpha detectors (Ortec Octete Plus with 450 mm^2 ULTRA-AS Detectors). After the initial deposition of polonium, residual 0.5 M HCl solutions were kept for about one year to form of ^{210}Po that was supported by ^{210}Pb [17]. Polonium caused by ^{210}Pb was kept in 0.5 HCl solution was plated again onto discs to determine the ^{210}Pb activity. Counting period was adjusted to keep the standard error under the 10% (relative standard error was approximately 5%). The Certified reference materials, IAEA-300 and IAEA-384, were analyzed to check the sensitivity of alpha spectrometry and recovery rates of standardized tracer for the sediment samples varying between 78 and 91%. Bateman equations and recovery were used to determine ^{210}Po (^{210}Pb) concentrations [15, 18].

In alpha spectrometric studies, ^{226}Ra activity is directly estimated from the layer with the lowest total ^{210}Pb activity. However, gamma spectroscopic studies are greatly likely to measure the concentrations of ^{226}Ra and ^{210}Pb separately for each layer.

The sediment core chronologies were obtained by the Constant Initial Concentration (CIC) and Constant Rate of Supply (CRS) models [19–25]. It was then evaluated which model was the best considering the model assumptions. CIC model supposes that an increased flux of sedimentary particles from the water column would remove proportionally increased amounts of ^{210}Pb from the water to the sediments, under the assumption of which sediments would have the same initial unsupported ^{210}Pb concentration irrespective of any variations in sediment accumulation rate. If the assumptions of the CIC model are satisfied, the

Fig. 1 Study area and sampling locations

unsupported ^{210}Pb activity will decay with depth in accordance with the below equation,

$$C(m) = C(0)e^{-\lambda t} \quad (1)$$

where $C(m)$ is the unsupported ^{210}Pb concentration at depth m and $C(0)$ the unsupported ^{210}Pb concentration of sediments at the sediment water interface. The age of a sediment layer with ^{210}Pb concentration $C(m)$ is thus obtained from below equation.

$$t = \frac{1}{\lambda} ln \left[\frac{C(0)}{C(m)} \right] \quad (2)$$

If the CIC model is applicable, the unsupported ^{210}Pb concentration must show a monotonic decline with depth and the total cumulative residual unsupported ^{210}Pb in sediment cores from the same area would vary roughly in proportion to the mean sediment accumulation rate [26].

However, CRS model assumes that there is a constant rate of supply of ^{210}Pb from the atmosphere to the lake waters resulting in a constant rate of supply of ^{210}Pb to the sediment regardless of any variations which may have occurred in the sediment accumulation rate [26]. Thus the age of each layer is calculated as follows:

$$t = \frac{1}{\lambda} ln \left[\frac{A(0)}{A(0) - A(m)} \right] \quad (3)$$

where $A(0)$ is the total inventory in core, λ the decay constant and $A(m)$ the cumulative inventory of unsupported ^{210}Pb concentrations at depth m. Accumulated and total inventory of ^{210}Pb are calculated as follows:

$$A(m) = \int_0^n C(m)M(m)dm,\ A(0) = \int_0^\infty C(m)M(m)dm \quad (4)$$

where, $C(m)$ is unsupported ^{210}Pb concentration (mBq g^{-1}), $M(m)$ is mass depth of core layer (g cm^{-2}).

$$\emptyset = A(0)\lambda \quad (5)$$

where $\varnothing$ is unsupported ^{210}Pb flux (mBq cm^{-2} year^{-1}) and calculated as above.

If the CRS model is applicable, non-monotonic profiles may be expected in response to major changes in the accumulation rate and different cores from the same area will have comparable ^{210}Pb residuals despite differences in the accumulation rates [26].

To improve the precision of sedimentation rate values, residence time of ^{210}Pb was calculated. Kumar et al. [27] thoroughly described how residence time of ^{210}Pb is calculated by the first order kinetic relationship.

$$dI_w/dt = \Phi_w - \{[\lambda_{Pb} + (1/T_w)]I_w\} \quad (6)$$

$$dI_s/dt = \Phi_s - \{[\lambda_{Pb} + (1/T_s)]I_s\} \quad (7)$$

where Φ_w and Φ_s represent the fluxes of ^{210}Pb in water and sediment, respectively. Similarly, I_w and I_s represent the inventories, λ_{Pb} is the radioactive decay constant of ^{210}Pb, T_w and T_s which are the residence times of the ^{210}Pb in water and sediment, respectively. Calculation details and necessary evaluations are in the article by Kumar et al. [27].

Metals and lead isotopes

Role of the heavy metals due to human activities or natural contributions is an important impact on environment. Therefore, researches on pollution are crucial part of geochemical studies [28, 29]. Nieboer and Richardson [30] claim that some heavy metals are constituents inherent in the marine environment. Fe, Cu, Zn, Co, Mn, Cr, Mo, V, Se and Ni are known to be essential to marine organisms which always function in combination with organic molecules in general proteins. However, Ag, Hg, Cu, Cd and Pb are particularly toxic [31]. Thus pollution levels and impacts of elements on environment are generally evaluated by four pollution indices of pollutants which are Enrichment Factor (EF), Anthropogenic Factor (AF), Pollution Load Index (PLI) and Geo-accumulation Index (I_{geo}). Enrichment factor is an effective tool especially to assess the magnitude of contaminants in the environment. The factor was initially developed to investigate the elements which stem from by precipitation in the atmosphere or seawater then it was extended to other environmental materials for instance soils, sediments, peats, tailings etc. [32]. Calculation of EF is based on the normalization in which Al, Sc, Fe, Zr are widely employed. Al is a common choice [15, 33, 34] to clarify EFs, also compensating the fluctuation on both particle size and sediment matrix in coastal sediments [28]. Fe is widely used in normalization as well as Al [35, 36] but some authors such as Din (1992) [37] and Rubio et al. [38] have argued that Fe originates from anthropogenic pollution [39]. Moreover, Sc and Zr are successfully utilized in the processes [40]. Zr is also known as relatively immobile and not emitted by human activities in practice. EF value is calculated by the formula below [41, 42]:

$$EF = (C_X/C_{Fe})_S/(C_X/C_{Fe})_C \quad (8)$$

where X is any element, C_X/C_{Fe} the concentration ratio of X to Fe, index (S) surface layer of sediment column and index (C) Earth crust. In addition, the background values in general could be immediately obtained from the bottom layer [28]. Nolting et al. [43] argues that EF would indicate that sediment is polluted if it is over 10. However, other authors [44, 45] suggest that If EFs varied 0.5 and 2.0 sediments would be independent of human impacts. On the other hand, the fact that they are over 2.0 implies significant anthropogenic inputs [39]. Anthropogenic factor (AF) is used to find the contamination level of a metal and its related values were obtained by the formula below [42];

$$AF = C_s/C_d \quad (9)$$

where C_s is the surface layer concentration and C_d the bottom layer concentration of sediment column [46]. Anthropogenic factor is also known as Contamination Factor (CF) [32, 47], where C_d value identified as the 30th layer of sediment column [15]. Contamination factor generally is used in combination with Pollution Load Index (PLI) in assessing metal pollution. According to Tomlinson et al. (1980) [48]

$$PLI = \sqrt[n]{CF_1 CF_2 \ldots CF_n} \quad (10)$$

For a site where CF is contamination factor and n number of metals,

$$PLI = \sqrt[n]{site_1 site_2 \ldots site_n} \quad (11)$$

where n is the number of sites for a zone [32]. PLI provides an idea to evaluate a site or zone quality. If PLI is 0.0, it shows perfect quality, 1.0 that there is only starting level pollution present and > 1 progressive deterioration of the zone. Geo-accumulation index is used to determine and describe the metal contamination in sediments by comparing present concentrations with pre-industrial ones as below:

$$I_{geo} = log_2\left(\frac{C_n}{1.5B_n}\right) \quad (12)$$

where C_n is the measured concentration of heavy metals in sediments, B_n the geochemical background value in average shale of element n and 1.5 the background matrix correlation [36]. Metal concentrations and stable Lead-isotopes (^{206}Pb, ^{207}Pb) were determined by ICP-MS (Perkin Elmer LN 900) spectrometry for selected samples. Prepared samples were digested with a modified Aqua Regia solution of equal parts concentrated HCl, HNO_3 and DIH_2O for 1 h in a heating block or hot water bath. Samples were prepared up to a volume with dilute HCl and separated of 0.5 g, 15 g, 30 g to be analyzed in ACME laboratory (ACME Anal. ISO 9002 Accredited Canadian Lab., Canada) (Method Description code is AQ250 2015_1 Bureau Veritas). As a quality assurance, it is declared that DS9, NIST-981-1Y, NIST-983-1Y standards were used in determination of element concentrations.

Results and discussions

Radionuclide concentrations

Vertical distribution of total ^{210}Pb activities ranges from 100.32 ± 7.56 Bq kg^{-1} to 40.55 ± 4.12 Bq kg^{-1} along the core IST-8 (Fig. 2b). In a similar way, it ranges from 108.59 ± 6.08 Bq kg^{-1} to 42.38 ± 3.43 Bq kg^{-1} along the core IST-2 (Fig. 2a). The total ^{210}Pb activity decreases from layer with maximum value to layer with minimum value, plateauing along the core. The lowest activity of total ^{210}Pb is named ^{226}Ra activity. Thus, determination of

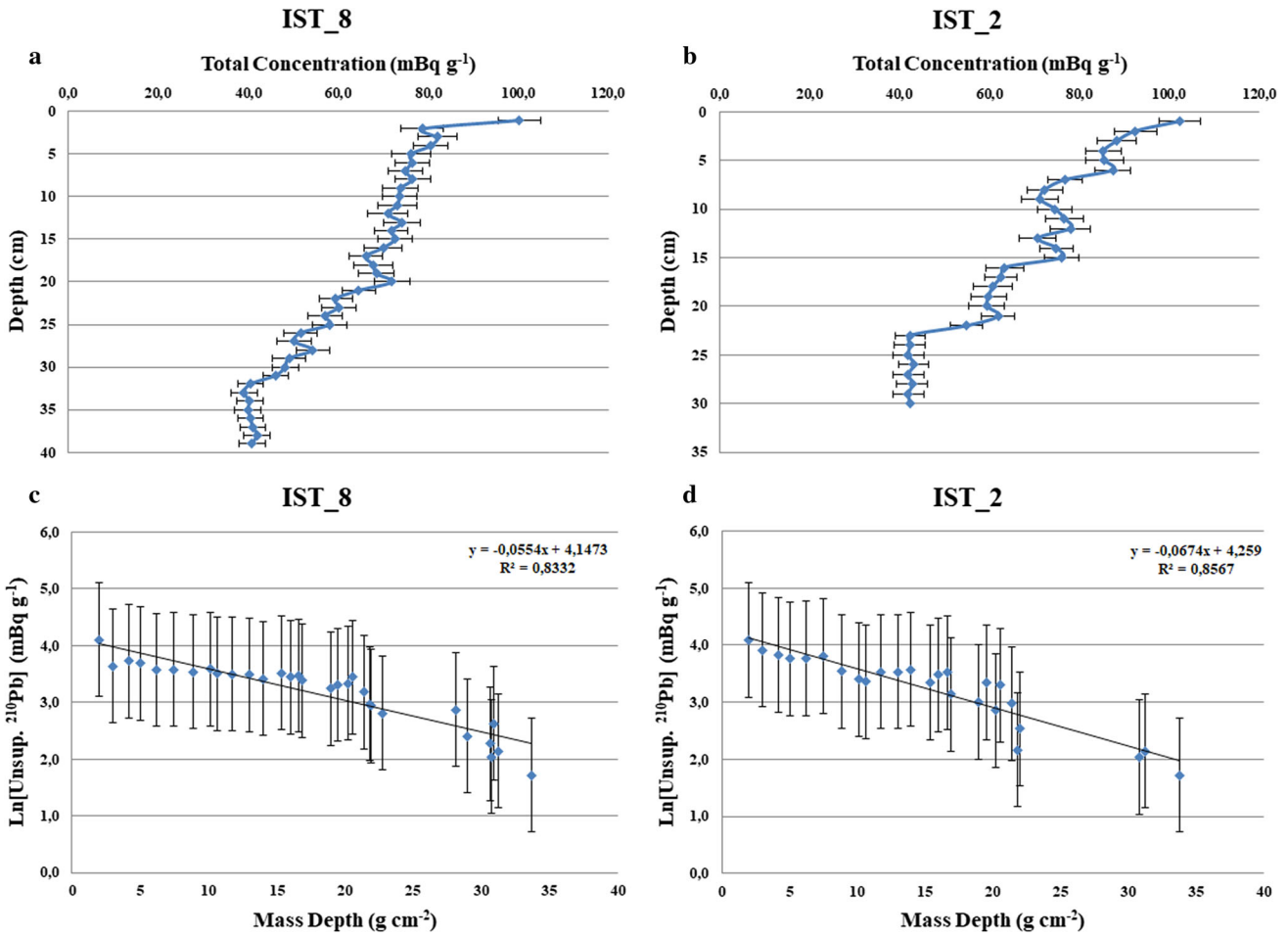

Fig. 2 Vertical distribution of total ^{210}Pb concentrations and plots of unsupported ^{210}Pb concentrations on a logarithmic scale versus mass depth in IST-2, IST-8 stations. Mass depths were calculated using the relationship with water content sediment pore. $MassDepth = D\rho_w/[1/(DW\%) + \rho_w/\rho_{dsed} - 1]$, where D indicates the linear depth, DW describes the dry weight of sediment, ρ_w and ρ_{dsed} are density of water and dry sediment, respectively. Values R^2 (0.83 for IST_2 and 0.85 for IST_8) seen on the upper right side of the graph **c** and graph **d** are lower than 0.95 thus model was not used in calculation of the sedimentation rates CF;CS (Constant flux; Constant sedimentation rates)

dating employs the part of the core between the layer with maximum activity of ^{210}Pb value and the one of minimum value, plateau part of the core is ignored [49]. As aforementioned, ^{226}Ra activities were determined as 40.55 ± 4.12 and 42.38 ± 3.43 Bq kg^{-1} in IST-8, IST-2 respectively. ^{226}Ra activity is also known as supported ^{210}Pb activity. In determination of dating, unsupported ^{210}Pb activities are used which are calculated by subtracting supported ^{210}Pb activity from the total ^{210}Pb activity in each layer.

From the vertical distribution of unsupported ^{210}Pb activities in IST-8 and IST-2 stations, it is follows that they do not obey to the exponential decrease from top to bottom along the core since values R^2 on the upper right in the Fig. 2c, d are lower than 0.95, in which case CF;CS model is obviously known not to be employed for those stations. Accordingly, applicability of CRS and CIC models were tested for cores. The residence times of ^{210}Pb were also calculated by utilizing profile distribution of ^{210}Pb activities as 2.4 year to correct dating processing. The residence time of ^{210}Pb in study area is lower than that of Mumbai Harbor Bay (40.87 year) [27].

Sedimentation rate ranges from 0.592 ± 0.022 to 0.036 ± 0.002 cm year^{-1} along the IST-8 core, displaying the increasing trend in time scale from 1850′s until today though not systematically increasing and also not displaying extremely high or low level sedimentation rates along the core. IST-8 station has a core depth of 30 cm corresponding to time scale between 1850's and 2010's (Fig. 3 and Supplementary material 1). Core inventory was determined as 7809.5 Bq m^{-2} thus ^{210}Pb flux was also calculated as 242.8 Bq m^{-2} year^{-1}. Average sedimentation rate is 0.315 ± 0.016 cm year^{-1} for both CRS and CIC models due to the value R^2 close to 0.95. Value R^2 is

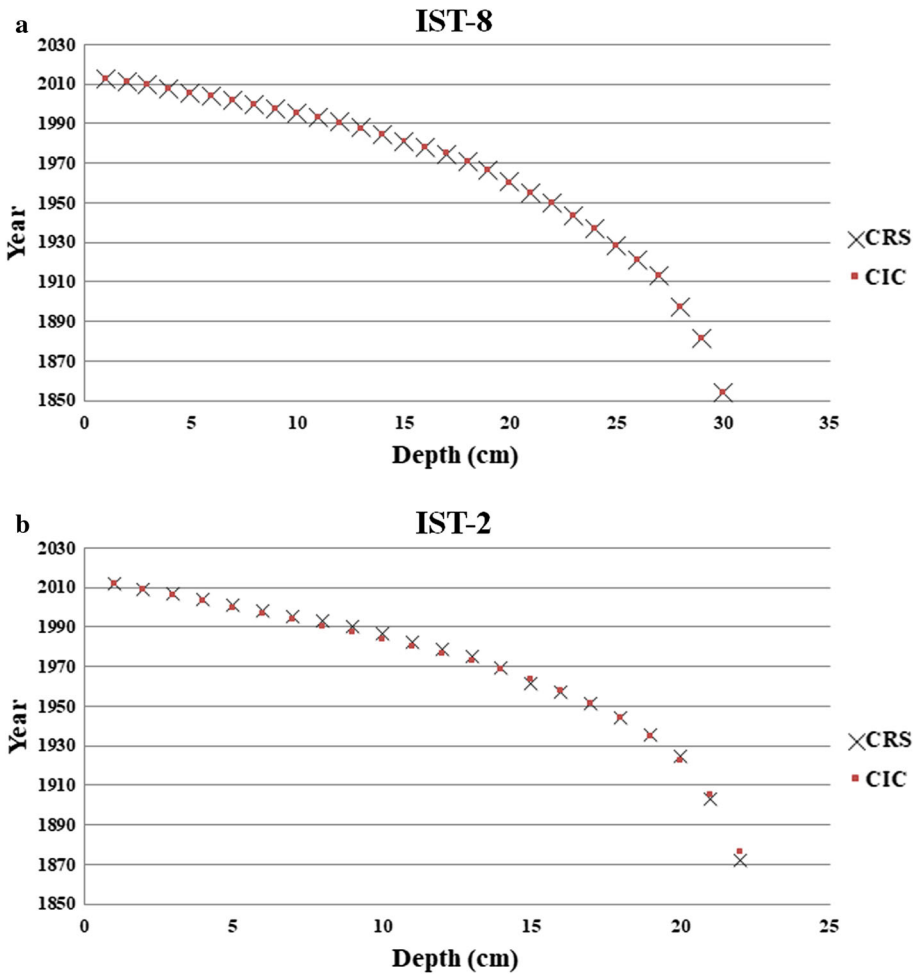

Fig. 3 Age-depth graphs for IST-8 and IST-2 stations

regression coefficient. It indicates the linearity between measured unsupported ^{210}Pb activities and exponential decrease with depth on semi log graph. If value R^2 is 1, core will be named as linear and linear cores give the same chronology in both CIC and CRS models [26]. In general, if value R^2 is 0.95 for a core, it is assumed as linear. Value R^2 of IST-8 is not far away from the 0.95, it is 0.83. In here, it should not be forgotten that according to CRS model, sedimentation rate is different in each layer but average value of CRS is one and according to CIC model average sedimentation rate is one value. It is possible that both models may have same average value. It may be aroused from the increases and decreases in sedimentation rates. Fluctuations on sedimentation rates may compensate the differences on average values and it may fix them to same value.

Sedimentation rate varies between 0.399 ± 0.011 and 0.032 ± 0.001 cm year^{-1} along the IST-2 core. Sedimentation pattern is similar to IST-8 but is not exactly same. IST-2 station has a core depth of 22 cm corresponding to time interval between 1870′s and 2010′s (Fig. 3 and Supplementary material 1). ^{210}Pb flux (205.9 Bq m^{-2} year^{-1}) was calculated using core inventory (6621.6 Bq m^{-2}). Average sedimentation rates in IST-2 are 0.251 ± 0.010 and 0.237 ± 0.011 cm year^{-1} both CRS and CIC models, respectively.

Maximum total ^{210}Pb activities are very close to each other but one core (IST-8) was obtained from Bakircay River mouth and the other one from the Ayvalik offshore in northern part of the Aegean Sea. Measured activities in study area are higher than in Mumbai Harbor Bay (48 Bq kg^{-1}) [27] and San Francisco Bay (33.3 Bq kg^{-1}) [50] but roughly the same as in Ribeira Bay (100 Bq kg^{-1}) [51] and lower than in Thermaikos Gulf (Eastern Mediterranean) (140 Bq kg^{-1}) [52].

Vertical distribution of unsupported ^{210}Pb activities are crucial for choosing mathematical model and pointing out the sedimentation pattern. Sedimentation patterns display almost the same in character on both stations. Therefore, ^{210}Pb fluxes calculated from core inventories are close to each other in study area. Therefore, it is seen that the best model for this study area is CRS because first of all cores display the non-monotonic decrease in depth. The second is that cores from different points within the same general

area have comparable total residual unsupported ^{210}Pb content. The last cores have similar ^{210}Pb fallout (^{210}Pb fluxes are close to each other in cores) from the atmosphere.

In general, ^{210}Pb flux around the world changes between 158 ± 113 and 20 ± 15 Bq m^{-2} year^{-1} from 0-10 North latitude to 70–80 North latitude, 117 and 2 ± 1 Bq m^{-2} year^{-1} from 0-10 South latitude to 80-90 south latitude in coastal, continental, ice-core and ocean samples [53]. ^{210}Pb fluxes calculated from the study area are higher than those from coastal locations in the Mediterranean area (75 Bq m^{-2} year^{-1}) [54], being roughly within the range of the world value of atmospheric ^{210}Pb flux (165–185 Bq m^{-2} year^{-1}) [26, 55]. Moreover, ^{210}Pb fluxes from the study area are higher than those of Gülbahçe Bay (173.6, 174.3, 160.5, 189.9, 135.3 and 206.9 Bq m^{-2} year^{-1}) [15].

Sedimentation rates in north Aegean Sea are lower than the ones in Mumbai Harbor Bay (0.52 ± 0.10, 0.73 ± 0.21, 1.12 ± 0.24 cm year^{-1}) [27], Thermaikos Gulf (0.88 ± 0.15, 0.75 ± 0.06, 0.48 ± 0.03 cm year^{-1}) [52], higher than in the Ribeira Bay (0.13 ± 0.02, 0.17 ± 0.02, 0.19 ± 0.01 cm year^{-1}) [51]. Sedimentation rates tend to increasing from bottom to top layers of the cores. They do not display continuously increasing trend but sedimentation trend of IST-8 is more stable than the one of IST-2. Average sedimentation rate in Bakircay River mouth is higher than the value of Ayvalik Offshore which is logical since Bakircay River has carried the continental materials down the seabed. Some high sedimentation rates have been seen in Ayvalik Offshore from past to nowadays. Such increases were observed especially in 1956, 1989, 1992, 2000 and 2008 years, which could not be related to the human processes or could not have originated from external inputs from the catchment area, since calculated ^{210}Pb flux in Ayvalik Offshore (205.9 Bq m^{-2} year^{-1}) is not significantly higher than the world average value of atmospheric ^{210}Pb flux (185 Bq m^{-2} year^{-1}). Clearly, if calculated value of ^{210}Pb flux there are supposed to be external inputs in the study area is higher than the world average value of atmospheric ^{210}Pb flux there will be outer inputs from the catchment area [56], which could be related to hydrothermal or seismic activity since north Aegean Sea has dynamic hydrothermal and seismic activities [9].

Metal concentrations

Element concentrations were not only measured in vertical sediment cores but also measured in surficial sediment samples (Fig. 4 and Supplementary Material 2) which showed Ca > Al % level, Mn > Ba > Cr > Zn > Ni > Pb > Cu ppm level and Hg ppb level order in surficial samples which consistent of 15 sampling points from Ayvalik to Izmir Bay in north Aegean Sea. A15 (inner part of the Izmir Bay), A14 (Gediz basin), A13 (Uzun Island) sampling points have highest element concentrations in terms of almost all elements, which could be related to maritime traffic or material influxes from Gediz basin, since Izmir Harbor is located in the inner part of the Izmir Bay and Gediz basin could also be responsible for high levels of element concentrations. Conversely in terms of Ba, Cr, Cu, Pb, Hg, A5 (Ayvalik offshore 2) sampling point, Mn, Zn, A7 (Dikili offshore) sampling point, and Al, Ni, A2 (Ayvalik offshore) sampling points have lowest concentrations. This surficial distribution of element concentration implies that A13, A15 stations are rich in Al, Ni and A14, A3 (Karaagac River mouth) stations are also rich in Al but station A2 is poor in them. Elements (Al, Ni) originate from terrigenous supply and it could be said that these stations do not display any pollution in terms of cited elements. Potentially, Karaagac River could be responsible for terrigenous materials. Ca and Ba from biogenic debris. A2, A11 (Foca nearshore), A7, A12 (Karaburun) and A10 (Foca offshore) stations show high level of Ca concentrations and A8 (Candarli nearshore), A15, A14 stations show high level of Ba concentrations which is more probably related to hydrothermal activity since hydrothermal zones have high biogenic affiliations [9]. Therefore, the stations above must be near the hydrothermal vents and Aegean Sea is known to have many hydrothermal areas. Mn is responsible for a group of micro earthquakes. A15, A10 (Foca offshore), A9 (Candarli offshore), A13, A14 stations have high but A7 (Dikili offshore) station has low level in Mn concentrations, which is reasonable because Aegean Sea has evidently high level of seismic activity. Cr and Cu are known as less mobile during the rock weathering because of their lower solubility. Thus they are immobile and Cr is transported in refractory minerals such as quartz, ilmenite, chromite, zircon whereas Cu is in the organic matter or clay minerals. A14, A15, A13 and A12 stations have high Cr and Cu concentrations but A5 station is poor in such element concentrations. Pb and Hg are known to be toxic in particular. Stations A15, A2, A12 and A8 are rich in Hg whereas those A14, A15, A13 and A11 are high in Pb concentrations both of which are lower than the other in A5 (Fig. 5). Pb input to the aquatic environment is an important problem and it should be identified in terms of natural or anthropogenic. ^{206}Pb/^{207}Pb ratio is utilized for differentiation and determination of the Pb input which could be natural or anthropogenic. ^{206}Pb/^{207}Pb ratio is 1.2 in geologic sediments but is lower than the 1.2 in anthropogenic sediments [57, 58]. In addition Zn, Cu, Cr and Ni are known as essential for marine organisms which always function in combination with organic molecules in general proteins. Stations A14, A15 and A13 have high level of Zn

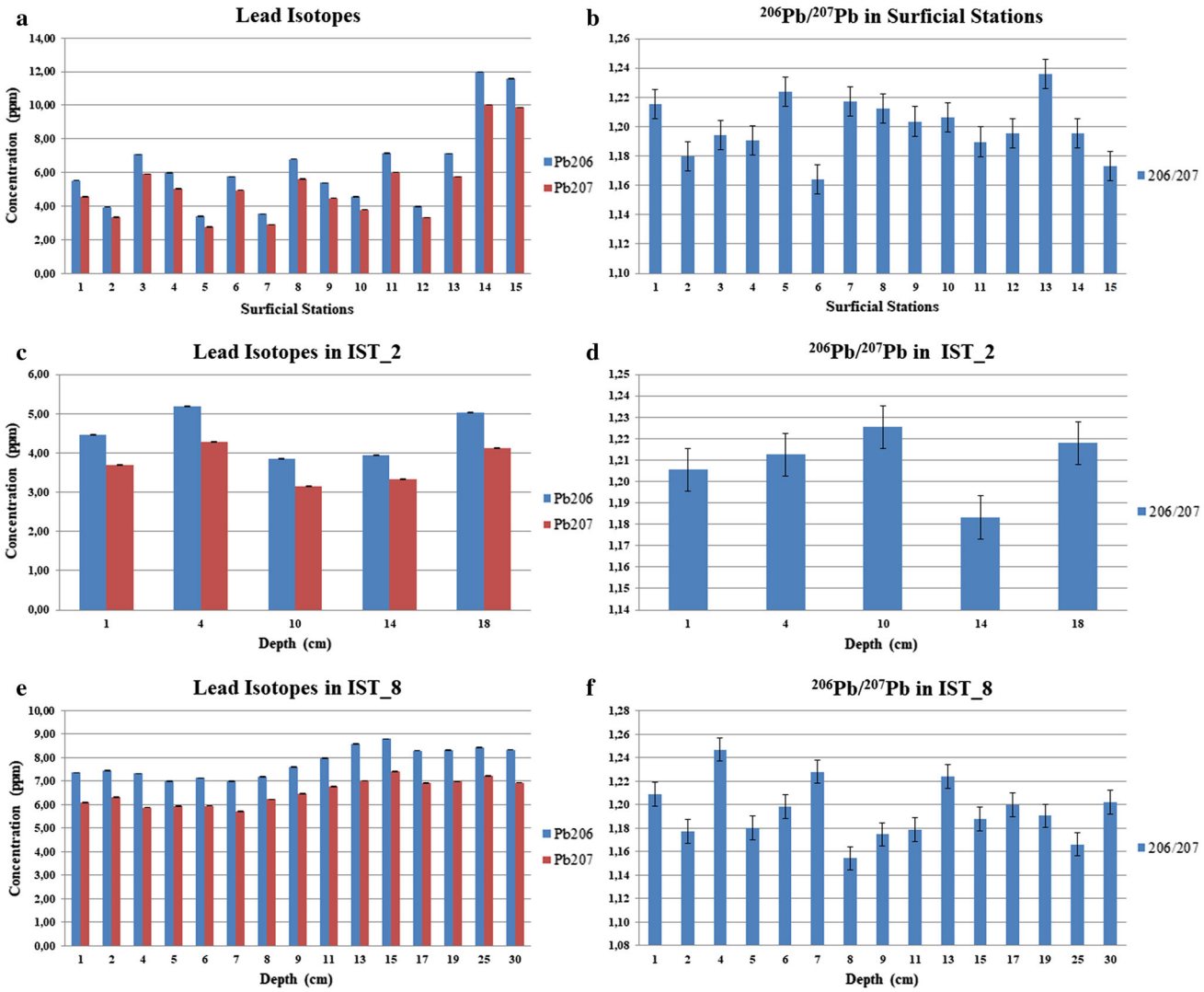

Fig. 4 Distribution of lead isotopes and lead isotope ratios in stations

concentrations whereas A7 has low level concentration of Zn. According to surficial distribution pattern of element concentrations, stations A2 and A12 display the same trend but they differ from the others in terms of pollution.

When glimpsed to the distribution of surficial $^{206}Pb/^{207}Pb$ ratios, it is seen that there are fifteen surficial stations along the Turkish coast in northern part of the Aegean Sea. In terms of $^{206}Pb/^{207}Pb$ ratio, five of them with error bars (A2, A4, A6, A11 and A15) have anthropogenic surficial sediments. A15 station displays high toxic (Pb, Hg) and biogenic (Ba) pollution. $^{206}Pb/^{207}Pb$ ratio also supports the sediment pollution in A15. In relation with the high level toxic and biogenic debris, A2, A4, A6, A11 stations have also displayed sediment pollution (lower values than 1.2) in terms of $^{206}Pb/^{207}Pb$ ratio.

In addition to surficial samples, vertical samples IST-2 and IST-8 were obtained from the Ayvalik offshore and the Candarli nearshore (Bakircay River mouth), respectively (Fig. 6). Considering Enrichment Factor (EF) values, Ayvalik offshore core has rich Ca (3.89), Mn (1.84), Zn (1.57), Pb (1.69), Hg (4.53) concentrations (Table 1) but in terms of Contamination Factor (CF) IST-2 station displays Ca (1.92) and Hg (2.40) pollutions (Table 2) whereas Bakircay River Mouth (IST-8) interestingly shows only Ca pollution in both contamination (1.78) and enrichment (1.98) factors. Enrichments were extensively seen in 2012. Furthermore, Ca displayed high EF values between 1968 and 2012 in IST-2 station but Ca displayed high EF values between 1995 and 2012 in IST-8 station too. Both Ayvalik offshore and Bakircay River Mouth have shown a starting level pollution from past until today while IST-2 showed an progressive deterioration in 2004 in terms of Pollution Load Index (PLI). In terms of Geo-accumulation Index, any metal concentration is evaluated in such a way that if Geo-accumulation Index is equal or under the zero, sediment will not be polluted by cited metal and if Geo-

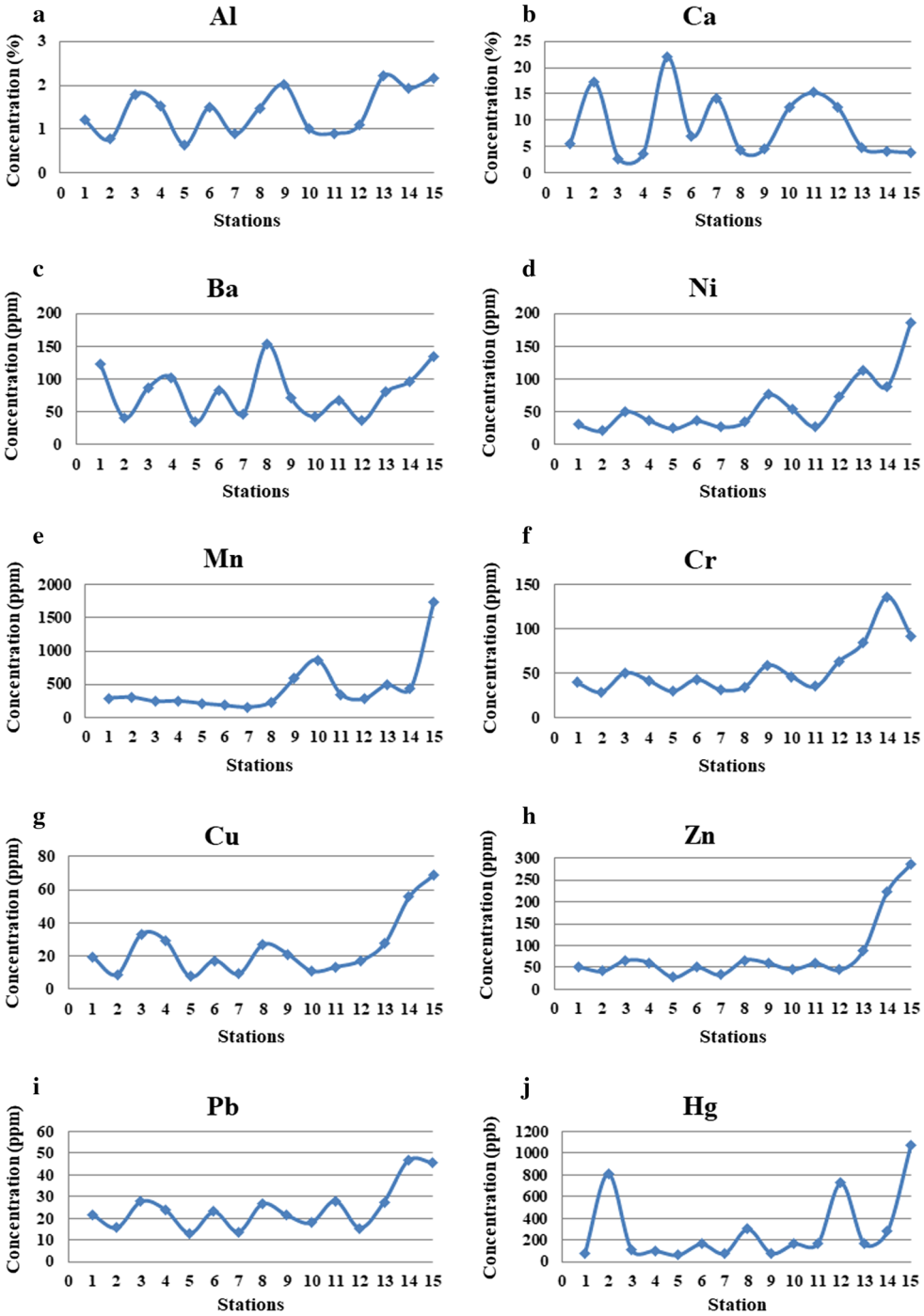

Fig. 5 Element concentrations in surficial samples

accumulation Index is between zero and one, sediment will be classified as "unpolluted to moderately polluted" [36]. It could be said that both Ayvalik offshore and Bakircay River Mouth stations are unpolluted by the above elements except by Ca and Hg. In terms of, Hg (0.68) IST-2 station has had the "unpolluted to moderately polluted" pollution degree since 2012, which has two time scales which correspond to "unpolluted to moderately polluted" pollution degree from 1984 to 2004 and from 2012 to nowadays in terms of Ca. Similarly, station IST-8 has also had "unpolluted to moderately polluted" pollution degree since 1995 (Table 3).

It is known that, Al is the lithogenous component of the sediment. Ni (0.941**), Mn (0.933**), Cr (0.882**), Cu (0.804**), Zn (0.880**), Pb (0.779**), Hg (0.879**) distributions have a correlation with Al distribution in Bakircay River Mouth but in Ayvalik offshore only Ba (0.973**), Ni (0.961**), Cr (0.917*), Cu (0.967**) show

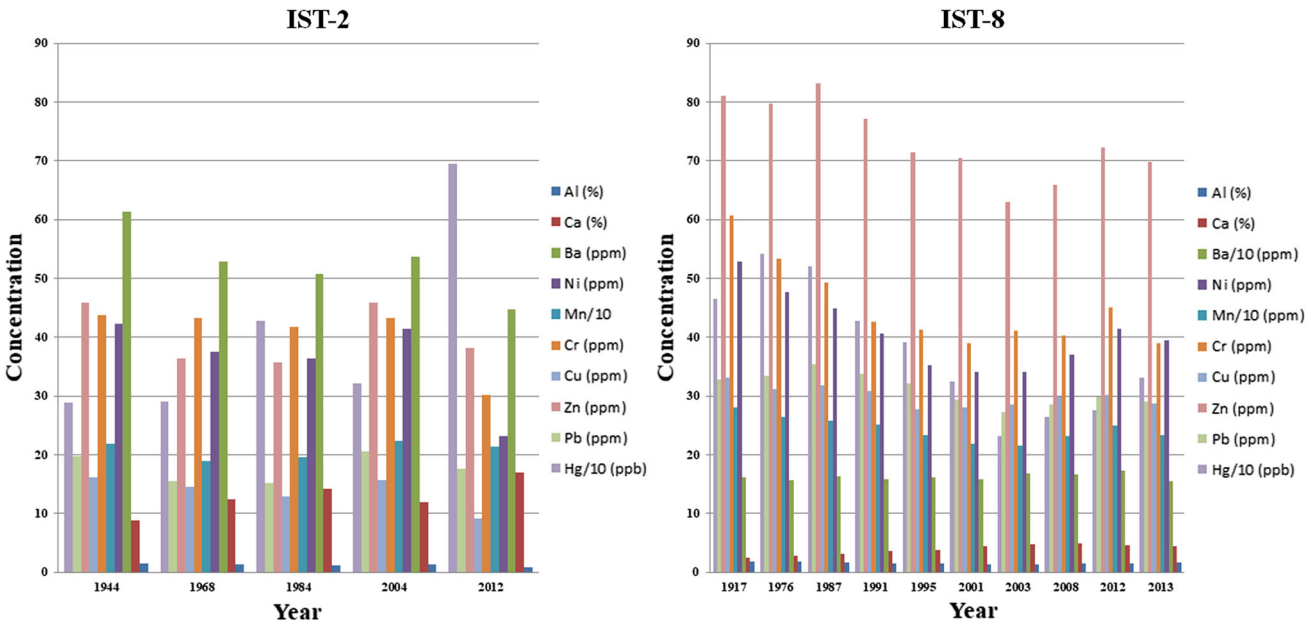

Fig. 6 Element concentrations in time scale for IST-2 and IST-8 stations

Table 1 Enrichment factors (EF) for IST-2 and IST-8 stations

	EF (Al)	EF (Ca)	EF (Ba)	EF (Ni)	EF (Mn)	EF (Cr)	EF (Cu)	EF (Zn)	EF (Pb)	EF (Hg)	Year
IST-2											
IST-2/1-2	1	3.89	1.38	1.03	1.84	1.30	1.06	1.57	1.69	4.53	2012
IST-2/4-5	1	1.70	1.02	1.15	1.20	1.16	1.13	1.17	1.22	1.30	2004
IST-2/10-11	1	2.22	1.06	1.10	1.15	1.22	1.02	1.00	0.99	1.89	1984
IST-2/14-15	1	1.83	1.05	1.08	1.05	1.20	1.09	0.96	0.96	1.22	1968
IST-2/18-19	1	1.07	1.00	1.00	1.00	1.00	1.00	1.00	1.00	1.00	1944
IST-8											
IST-8/1-2	1	1.98	1.07	0.83	0.93	0.72	0.97	0.96	0.98	0.79	2013
IST-8/2-3	1	2.11	1.21	0.89	1.01	0.84	1.03	1.01	1.03	0.67	2012
IST-8/4-5	1	2.44	1.25	0.85	1.01	0.81	1.10	0.99	1.05	0.69	2008
IST-8/5-6	1	2.50	1.25	0.89	1.06	0.85	1.15	1.02	1.09	0.67	2006
IST-8/6-7	1	2.52	1.32	0.88	1.02	0.87	1.11	1.04	1.09	0.64	2005
IST-8/7-8	1	2.58	1.40	0.86	1.03	0.91	1.15	1.04	1.11	0.66	2003
IST-8/8-9	1	2.27	1.24	0.81	0.98	0.81	1.07	1.09	1.12	0.88	2001
IST-8/9-10	1	2.10	1.25	0.83	0.98	0.80	1.07	1.09	1.23	0.89	1999
IST-8/11-12	1	1.85	1.22	0.82	1.02	0.83	1.03	1.08	1.20	1.03	1995
IST-8/13-14	1	1.64	1.11	0.87	1.02	0.80	1.06	1.08	1.17	1.04	1991
IST-8/15-16	1	1.29	1.04	0.87	0.94	0.84	0.99	1.05	1.11	1.15	1987
IST-8/17-18	1	1.22	1.06	0.85	0.94	0.88	0.95	0.96	1.05	1.08	1982
IST-8/19-20	1	1.13	0.98	0.91	0.95	0.89	0.95	0.99	1.03	1.18	1976
IST-8/25-26	1	1.04	0.96	0.89	0.96	0.93	0.94	0.94	1.03	1.25	1954
IST-8/30-31	1	1	1	1	1	1	1	1	1	1	1917

positive correlation with Al (**$p < 0.01$, *$p < 0.05$). From the correlations with Al, it is clear that concentrations of all elements are directly controlled by continental weathering except Ca and Br in station IST-8 (Table 4) which is an expected situation since Ca and Ba originate from biogenic debris. In addition to Ca, concentrations of some other

Table 2 Contamination Factor (CF) and pollution load index (PLI) values for IST-2 and IST-8 stations

	CF (Al)	CF (Ca)	CF (Ba)	CF (Ni)	CF (Mn)	CF (Cr)	CF (Cu)	CF (Zn)	CF (Pb)	CF (Hg)	PLI	Year
IST-2												
IST-2/1-2	0.53	1.92	0.73	0.55	0.98	0.69	0.56	0.83	0.89	2.40	0.88	2012
IST-2/4-5	0.85	1.36	0.87	0.98	1.02	0.99	0.97	1.00	1.05	1.11	1.01	2004
IST-2/10-11	0.78	1.61	0.83	0.86	0.89	0.95	0.80	0.78	0.77	1.48	0.94	1984
IST-2/14-15	0.82	1.40	0.86	0.89	0.86	0.99	0.90	0.79	0.79	1.00	0.92	1968
IST-2/18-19	1	1	1	1	1	1	1	1	1	1	1	1944
IST-8												
IST-8/1-2	0.90	1.78	0.96	0.74	0.83	0.64	0.87	0.86	0.88	0.71	0.88	2013
IST-8/2-3	0.89	1.87	1.07	0.78	0.89	0.74	0.91	0.89	0.91	0.59	0.91	2012
IST-8/4-5	0.82	2.00	1.03	0.70	0.83	0.67	0.90	0.81	0.87	0.57	0.87	2008
IST-8/5-6	0.79	1.99	0.99	0.71	0.84	0.67	0.91	0.81	0.87	0.53	0.86	2006
IST-8/6-7	0.79	1.99	1.04	0.70	0.81	0.69	0.88	0.82	0.86	0.51	0.85	2005
IST-8/7-8	0.75	1.93	1.05	0.64	0.77	0.68	0.86	0.78	0.83	0.50	0.82	2003
IST-8/8-9	0.79	1.80	0.98	0.64	0.78	0.64	0.85	0.87	0.89	0.70	0.86	2001
IST-8/9-10	0.78	1.63	0.97	0.64	0.76	0.63	0.83	0.85	0.95	0.69	0.84	1999
IST-8/11-12	0.82	1.51	1.00	0.67	0.83	0.68	0.84	0.88	0.98	0.84	0.88	1995
IST-8/13-14	0.88	1.44	0.98	0.77	0.90	0.70	0.93	0.95	1.03	0.92	0.93	1991
IST-8/15-16	0.97	1.25	1.01	0.85	0.92	0.81	0.96	1.02	1.08	1.12	0.99	1987
IST-8/17-18	0.96	1.18	1.01	0.81	0.90	0.84	0.91	0.93	1.00	1.04	0.95	1982
IST-8/19-20	0.99	1.12	0.97	0.90	0.94	0.88	0.94	0.98	1.02	1.16	0.99	1976
IST-8/25-26	1.01	1.04	0.97	0.89	0.97	0.94	0.95	0.95	1.04	1.26	1.00	1954
IST-8/30-31	1	1	1	1	1	1	1	1	1	1	1	1917

elements are also not directly controlled by continental weathering, for instance Mn, Zn, Pb, Hg in station IST-2. It is also reasonable because potentially Bakircay River may bring the continental weathering materials from stream bed to river mouth. Concentration of Ca interestingly displays negative correlations with the rest in both stations. The trend for Ni has closely been followed by the trend for Cr and Cu in the same way but it has no correlation with Zn, Pb and Hg in Ayvalik offshore. Ni, Cr and Cu are probably derived from the same source or sources, which is necessary because they are known to be essential to marine organisms. Pb and Hg are particularly toxic so their sources are apart from the Ni, Cr, Cu ones in Ayvalik offshore whereas Pb and Hg show correlations with Ni, Cr and Cu in station IST-8 which indicates that Bakircay River contributes to concentrations of Pb and Hg in aquatic environment. In general, element concentrations have decreased from past to nowadays in both IST-2 and IST-8 but elevated element concentrations have not been seen. However, Ca concentrations have increased since 1917 in station Bakircay River Mouth and Ca, Hg concentrations have increased since 1944 in station Ayvalik offshore.

When glimpsed to the relation between EF of some elements and profile distribution of $^{206}Pb/^{207}Pb$ ratio in core IST-2, it is seen that EF values for Ca, Ba, Ni, Mn, Cr, Cu and Hg are higher than 1 in 1968 and also $^{206}Pb/^{207}Pb$ ratio indices sediment pollution in same year. It is possible to see similar relations between EF values (Table 1) and $^{206}Pb/^{207}Pb$ ratios (Supplementary Material 2) in 2012–2009, 2007–2006, 2002–1992, 1990–1983, 1982–1918 years respectively for core IST-8. However there is no relation between profile distribution of unsupported ^{210}Pb activity (Fig. 2) and ^{206}Pb concentrations (Supplementary Material 2) in both IST-2, IST-8 cores.

Conclusions

Present study has tried to describe historical evaluation of north Aegean Sea in Turkish coast. To achieve a general idea for study area, first of all vertical distributions of ^{210}Pb activity concentrations were determined by alpha spectroscopy, which shows that maximum unsupported ^{210}Pb concentrations are the same in each core and they compatible with other part of the Aegean Sea [15]. It could be said that ^{210}Pb depositions to the Ayvalik Offshore and Bakircay River Mouth stations are systematic and do not display exponential decrease from top to bottom layers.

Table 3 Geo-accumulation Index (Igeo) for IST-2 and IST-8 stations

Igeo	Al	Ca	Ba	Ni	Mn	Cr	Cu	Zn	Pb	Hg	Year
IST-2											
IST-2/1-2	− 1.50	0.36	− 1.04	− 1.46	− 0.62	− 1.12	− 1.41	− 0.85	− 0.75	0.68	2012
IST-2/4-5	− 0.81	− 0.15	− 0.78	− 0.61	− 0.55	− 0.60	− 0.63	− 0.58	− 0.52	− 0.43	2004
IST-2/10-11	− 0.94	0.11	− 0.86	− 0.81	− 0.75	− 0.65	− 0.91	− 0.94	− 0.96	− 0.02	1984
IST-2/14-15	− 0.87	− 0.10	− 0.80	− 0.76	− 0.80	− 0.60	− 0.74	− 0.92	− 0.93	− 0.58	1968
IST-2/18-19	− 0.58	− 0.58	− 0.58	− 0.58	− 0.58	− 0.58	− 0.58	− 0.58	− 0.58	− 0.58	1944
IST-8											
IST-8/1-2	− 0.74	0.24	− 0.65	− 1.01	− 0.85	− 1.22	− 0.79	− 0.80	− 0.76	− 1.08	2013
IST-8/2-3	− 0.76	0.32	− 0.49	− 0.94	− 0.75	− 1.01	− 0.72	− 0.75	− 0.72	− 1.34	2012
IST-8/4-5	− 0.87	0.42	− 0.55	− 1.10	− 0.86	− 1.17	− 0.73	− 0.88	− 0.79	− 1.40	2008
IST-8/5-6	− 0.92	0.41	− 0.60	− 1.08	− 0.83	− 1.16	− 0.72	− 0.89	− 0.79	− 1.50	2006
IST-8/6-7	− 0.93	0.41	− 0.52	− 1.11	− 0.89	− 1.13	− 0.77	− 0.88	− 0.81	− 1.56	2005
IST-8/7-8	− 1.00	0.37	− 0.52	− 1.22	− 0.96	− 1.15	− 0.80	− 0.95	− 0.85	− 1.59	2003
IST-8/8-9	− 0.92	0.27	− 0.61	− 1.22	− 0.95	− 1.22	− 0.82	− 0.79	− 0.75	− 1.10	2001
IST-8/9-10	− 0.95	0.12	− 0.63	− 1.22	− 0.97	− 1.26	− 0.85	− 0.82	− 0.65	− 1.12	1999
IST-8/11-12	− 0.88	0.01	− 0.59	− 1.17	− 0.85	− 1.14	− 0.84	− 0.77	− 0.62	− 0.84	1995
IST-8/13-14	− 0.77	− 0.06	− 0.62	− 0.97	− 0.74	− 1.09	− 0.69	− 0.66	− 0.54	− 0.71	1991
IST-8/15-16	− 0.63	− 0.26	− 0.57	− 0.82	− 0.71	− 0.88	− 0.64	− 0.55	− 0.48	− 0.42	1987
IST-8/17-18	− 0.64	− 0.35	− 0.56	− 0.88	− 0.73	− 0.83	− 0.72	− 0.70	− 0.58	− 0.53	1982
IST-8/19-20	− 0.60	− 0.42	− 0.63	− 0.74	− 0.67	− 0.77	− 0.67	− 0.61	− 0.56	− 0.37	1976
IST-8/25-26	− 0.58	− 0.52	− 0.63	− 0.75	− 0.63	− 0.68	− 0.67	− 0.67	− 0.53	− 0.25	1954
IST-8/30-31	− 0.58	− 0.58	− 0.58	− 0.58	− 0.58	− 0.58	− 0.58	− 0.58	− 0.58	− 0.58	1917

Thus in calculation of sedimentation rates, applicability of CRS and CIC mathematical models were tested and it is decided that the best model is CRS for study area. ^{210}Pb fluxes from core inventories are close to each other and they are almost within the range of the global atmospheric ^{210}Pb flux value. However, ^{210}Pb flux from Bakircay River Mouth is a little higher than the Ayvalik Offshore and the global atmospheric fluxes, which is logical since if measured ^{210}Pb flux is higher than the atmospheric supply rates, there would be external inputs from the near catchment area [56]. It could be argued that ^{210}Pb flux has been accounted for by the material from the river. In addition, sedimentation rates along the cores display irregular increases and decreases in stations of Ayvalik Offshore and Bakircay River Mouth. Station Bakircay River Mouth has two effects which may be related to irregularity on sedimentation pattern. The first one is Ba concentration. It is known that, high level of Ba concentration indicates the biogenic debris (possible hydrothermal activity) [8]. The second one is the inputs from the river to sediment accumulation area. Thus, average sedimentation rate (0.315 ± 0.014 cm year^{-1}) in Bakircay River Mouth station is higher than in the Ayvalik Offshore one (0.215 ± 0.009 cm year^{-1}). However, station Ayvalik Offshore has no obvious effect related to irregular sedimentation pattern. The residence time of ^{210}Pb was also calculated by profile distribution of ^{210}Pb activity concentrations in the core which was found to be 2.4 years and sediment dating was corrected via residence time of ^{210}Pb.

Pollution level in the study area was evaluated by means of four pollution index and results were supported in terms of lead isotopes (^{206}Pb/^{207}Pb ratio). Some element concentrations have high level in the surficial sediment samples, more or less half of the study area is polluted in terms of measured elements. In addition, Lead-isotope ratio supports the polluted decision in surficial samples especially stations A2, A4, A6, A11 and A15 (Fig. 4b). As to core samples, some elements display high level concentrations but Ca and Hg pollutions exist in Ayvalik Offshore station and only Ca pollution exists in Bakircay River Mouth. While Ayvalik Offshore displayed Ca pollution between 1968 and 2012, Bakircay River Mouth showed Ca pollution from 1995 to 2012 in terms of enrichment and contamination factors. Moreover, profile distributions of ^{206}Pb/^{207}Pb ratio support the sediment pollutions between mentioned years in both cores. Under the Pollution Load Index, Ayvalik offshore and Bakircay River Mouth have both shown a starting level pollution through decades but

Table 4 Correlation coefficients between element concentrations for surficial and core samples

	Al	Ca	Ba	Ni	Mn	Cr	Cu	Zn	Pb	Hg
ist8										
Al	1									
Ca	− 0.865**	1								
Ba	− 0.275	0.429	1							
Ni	0.941**	− 0.813**	− 0.170	1						
Mn	0.933**	− 0.811**	− 0.152	0.968**	1					
Cr	0.882**	− 0.854**	− 0.094	0.945**	0.919**	1				
Cu	0.804**	− 0.636*	− 0.011	0.913**	0.913**	0.835**	1			
Zn	0.880**	− 0.887**	− 0.308	0.829**	0.840**	0.765**	0.743**	1		
Pb	0.779**	− 0.903**	− 0.397	0.672**	0.732**	0.664**	0.584*	0.920**	1	
Hg	0.879**	− 0.958**	− 0.486	0.762**	0.788**	0.784**	0.609*	0.889**	0.927**	1
ist2										
Al	1									
Ca	− 0.975**	1								
Ba	0.973**	− 0.992**	1							
Ni	0.961**	− 0.901*	0.878	1						
Mn	0.123	− 0.227	0.225	0.102	1					
Cr	0.917*	− 0.828	0.803	0.970**	− 0.141	1				
Cu	0.967**	− 0.943*	0.910*	0.985**	0.146	0.943*	1			
Zn	0.574	− 0.663	0.644	0.546	0.872	0.329	0.603	1		
Pb	0.350	− 0.460	0.433	0.340	0.951*	0.109	0.406	0.967**	1	
Hg	− 0.927*	0.881*	− 0.842	− 0.960**	0.100	− 0.978**	− 0.968**	− 0.392	− 0.181	1
Surface										
Al	1									
Ca	− 0.866**	1								
Ba	0.582*	− 0.766**	1							
Ni	0.731**	− 0.463	0.338	1						
Mn	0.453	− 0.248	0.287	0.846**	1					
Cr	0.703**	− 0.492	0.259	0.753**	0.458	1				
Cu	0.759**	− 0.677**	0.659**	0.804**	0.641*	0.795**	1			
Zn	0.631*	− 0.465	0.520*	0.836**	0.746**	0.813**	0.948**	1		
Pb	0.717**	− 0.622*	0.649**	0.694**	0.559*	0.796**	0.934**	0.921**	1	
Hg	0.068	0.038	0.096	0.559*	0.585*	0.282	0.430	0.535*	0.308	1

*$p < 0.05$; **$p < 0.01$

Ayvalik Offshore displayed an progressive deterioration in 2004. Considering Geo-accumulation Index, both stations have Ca and Hg pollutions. While Ayvalik Offshore station has had the "unpolluted to moderately polluted" pollution degree since 2012, Bakircay River Mouth has had the "unpolluted to moderately polluted" pollution degree since 1995.

Acknowledgements This research work was supported by the Ege University Science and Technology Centre (EBİLTEM). Project number is 13NBE009. Author thanks to EBİLTEM.

References

1. Skliris N, Mantziafou A, Sofianos S, Gkanasos A (2010) Satellite-derived variability of the Aegean Sea ecohydrodynamics. Cont Shelf Res 30:403–418
2. Tsabaris C, Zervakis V, Kaberi H, Delfanti R, Georgopoulos D, Lampropoulou M, Kalfas CA (2014) ^{137}Cs vertical distribution at the deep basins of the North and Central Aegean Sea, Greece. J Environ Radioact 132:47–56
3. Dando PR, Aliani S, Arab H, Bianchi CN, Brehmer M, Cocito S, Fowler SW, Gundersen J, Hooper LE, Kölbl R, Kuever J, Linke P, Makropoulos KC, Meloni R, Miquel J-C, Morri C, Müller S, Robinson C, Schlesner H, Sievert S, Stöhr R, Stüben D, Thomm M, Varnavas SP, Ziebis W (2000) Hydrothermal studies in the Aegean Sea. Phys Chem Earth 25:1–8

4. Dando PR, Stüben D, Varnavas SP (1999) Hydrothermalism in the Mediterranean Sea. Prog Oceanogr 44:333–367
5. Poulos SE (2009) Origin and distribution of the terrigenous component of the unconsolidated surface sediment of the Aegean floor: a synthesis. Cont Shelf Res 29:2045–2060
6. Varnavas SP, Cronan DS (1991) Hydrothermal metallogenic processes off the islands of Nisiros and Kos in the Hellenic Volcanic Arc. Mar Geol 99:109–133
7. Bayhan E, Ergin M, Temel A, Keskin Ş (2001) Sedimentology and mineralogy of surficial bottom deposits from the Aegean–Çanakkale–Marmara transition (Eastern Mediterranean): effects of marine and terrestrial factors. Mar Geol 175:297–315
8. Makropoulos K, Kouskouna V, Karnassopoulos A, Dando P, Varnavas SP (2000) Seismicity in the hellenic volcanic arc hydrothermal system in relation to geochemical parameters. Phys Chem Earth B 25:19–23
9. Varnavas SP, Panagiotaras D, Megalovasilis P, Dando P, Alliani S, Meloni R (2000) Compositional characterization of suspended particulate metter in hellenic volcanic arc hydrothermal centres. Phys Chem Earth Part B 25(1):9–18
10. Sarı E, Çağatay MN (2001) Distribution of heavy metals in the surface sediments of the Gulf of Saros. Environ Int 26:169–173
11. Aloupi M, Angelidis MO (2001) Geochemistry of natural and anthropogenic metals in the coastal sediments of the Island of Lesvos, Aegean Sea. Environ Pollut 113:211–219
12. Boisson F, Miquel JC, Cotret O, Fowler SW (2001) 210Po and 210Pb cycling in an hydrothermal vent zone in the coastal Aegean Sea. Sci Total Environ 281:111–119
13. Ergin M, Kadir S, Keskin Ş, Turhan-Akyüz N, Yaşar D (2007) Late Quaternary climate and sea-level changes recorded in sediment composition off the Büyük Menderes River delta (eastern Aegean Sea, Turkey). Quatern Int 167:162–176
14. Otansev P, Taşkın H, Başsarı A, Varinlioğlu A (2016) Distribution and environmental impacts of heavy metals and radioactivity in sediment and sea water samples of Marmara Sea. Chemosphere 154:266–275
15. Sert I, Yener G, Ozel E, Pekcetinoz B, Eftelioglu M, Gorgun AU (2012) Estimation of sediment accumulation rates using naturally occuring 210Pb models in Gulbahce Bay, Aegean Sea, Turkey. J Environ Radioact 107:1–12
16. Flynn WW (1968) The determination of low levels of polonium-210 in environmental materials. Anal Chim Acta 43:221–227
17. Boisson F, Miquel JC, Cotret O, Fowler SW (2001) 210Po and 210Pb cycling in an hydrothermal vent zone in the coastal Aegean Sea. Sci Total Environ 281:111–119
18. Bateman H (1910) Solution of a system of differential equations occurring in the theory of radioactive transformations. Proc Camb Philos Soc 15:423–427
19. Walling DE, He Q, Appleby PG (2003) Conversion models for use in soil-erosion, soil-redistribution and sedimentation investigations. ss 111-164. Zapata, F., ed. 2003. Handbook for the assessment of soil erosion and sedimentation using environmental radionuclides. Springer Netherlands, 219 s
20. Sanches-cabeza JA, Ruiz-fernandez AC (2012) 210Pb sediment chronology: an integrated formulation and classification of dating models. Geochim Cosmochim Acta 82:183–200
21. Krishnaswami LD, Martin JM, Meybeck M (1971) Geochronology of lake sediments. Earth Planet Sci Lett 11:407–414
22. Koide M, Soutar A, Goldberg ED (1972) Marine geochronology with 210Pb. Earth Planet Sci Lett 14:442–446
23. Robbins JA, Krezosky JR, Mozley SC (1977) Radioactivity in sediments of the Great Lakes: post-depositional redistribution by deposit-feeding organisms. Earth Planet Sci Lett 36:325–333
24. Appleby PG, Oldfield F (1978) The calculation of lead-210 dates assuming a constant rate of supply of unsupported 210Pb to the sediment. CATENA 5:1–8
25. Oldfield F, Appleby PG, Battarbee RW (1978) Alternative 210Pb dating: results from the New Guinea Highlands and Lough Erne. Nature 271:339–342
26. Appleby PG, Oldfield F (1983) The assessment of 210Pb data from sites with varying sediment accumulation rates. Hydrobiologia 103:29–35
27. Kumar A, Rout S, Karpe R, Mishra MK, Narayanan U, Singhal RK, Ravi PM, Tripathi RM (2015) Inventory, fluxes and residence times from the depth profiles of naturally occurring ^{210}Pb in marine sediments of Mumbai Harbor Bay. Environ Earth Sci 73:4019–4031
28. Diaz-asencio M, Alonso-Hernández CM, Balanos-Álvarez Y, Gómez-Batista M, Pinto V, Morabito R, Hernández-Albernas JI, Eriksson M, Sanchez-Cabeza JA (2009) One century sedimentary record of Hg and Pb pollution in the Sagua estuary (Cuba) derived from 210Pb and 137Cs chronology. Mar Pollut Bull 59:108–115
29. Salomons W, Kertlik H, van Pagee H, Klomp R, Schreur A (1988) Behaviour and impact assessment of heavy metals in estuary and coastal zones. In: Seeliger U, de Lacerda LD, Patchineelam SR (eds) Metals in coastal environments of Latin America. Springer, Berlin
30. Nieboer E, Richardson DHS (1980) The replacement of the nondescript term 'heavy metals' by a biologically and chemically significant classification of metal ions. Environ Pollut B 1:3–26
31. Bryan GW (1979) Bioaccumulation of marine pollutants. Philos Trans R Soc Lond, Ser B 286:483–505
32. Goher ME, Farhat HI, Abdo MH, Salem SG (2014) Metal pollution assessment in the surface sediment of Lake Nasser, Egypt. Egypt J Aquat Res 40:213–224
33. Parsons MJ, Long DT, Yohn SS (2010) Assessing the natural recovery of a lake contaminated with Hg using estimated recovery rates determined by sediment chronologies. Appl Geochem 25:1676–1687
34. Chatterjee M, Silva FEV, Sarkar SK (2007) Distribution and possible source of trace elements in the sediment cores of a tropical macrotidal estuary and their ecotoxicological significance. Environ Int 33:346–356
35. Zakir HM, Shikazono N, Otomo K (2008) Geochemical distribution of trace metals and assessment of anthropogenic pollution in sediments of Old Nakagawa River. Tokyo Jpn Am J Environ Sci 4(6):661–672
36. El-Amier YA, Elnaggar AA, El-Alfy MA (2016) Evaluation and mapping spatial distribution of bottom sediment heavy metal contamination in Burullus Lake, Egypt. Egypt J Basic Appl Sci 4(1):55–66
37. Din ZB (1992) Use of aluminium to normalize heavy-metal data from estuarine and coastal sediments of Straits of Melaka. Mar Pollut Bull 24(10):484–491
38. Rubio B, Nombela M, Vilas F (2000) Geochemistry of major and trace elements in sediments of the Ria de Vigo (NW Spain): an assessment of metal pollution. Mar Pollut Bull 40:968–980
39. Shi Q, Leipe T, Rueckert P, Zhou D, Harff J (2010) Geochemical sources, deposition and enrichment of heavy metals in short sediment cores from the Pearl River Estuary, Southern China. J Mar Syst 82(Supp 1):28–42
40. Darwish MAG (2013) Geochemistry of the High Dam Lake sediments, south Egypt: implications for environmental significance. Int J Sedim Res 28:544–559
41. Qi S, Leipe T, Rueckert P, Di Z (2010) Geochemical sources, deposition and enrichment of heavy metals in short sediment cores from the Pearl River Estuary. South China J Mar Syst 82:28–42
42. Szefer P, Glasby GP, Kunzendorf H, Görlich EA, Latka K, Ikuta K, Ali A (1998) The distribution of rare earth and other elements and the mineralogy of the iron oxyhydroxide phase in marine

ferromanganese concretions from within Slupsk Furrow in the southern Baltic. Appl Geochem 13(3):305–312
43. Nolting RF, Ramkema A, Everaats JM (1999) The geochemistry of Cu, Cd, Zn, Ni and Pb in sediment cores from the continental slope of the Banc d'Arguin (Mauritania). Cont Shelf Res 19:665–691
44. Sutherland RA (2000) Bed sediment-associated trace metals in an urban stream, Oahu, Hawaii. Environ Geol 39:611–627
45. Liaghati T, Preda M, Cox M (2003) Heavy metal distribution and controlling factors within coastal plain sediments, bells creek catchments, Southeast Queensland, Australia. Environ Int 29:935–948
46. Glasby GP, Szefer P, Geldon J, Warzocha J (2004) Heavy-metal pollution of sediments from Szczecin Lagoon and the Gdansk Basin, Poland. Sci Total Environ 330:249–269
47. Hakanson L (1980) An ecological risk index for aquatic pollution control: a sedimentological approach. Water Res 14:975–1001
48. Tomlinson DC, Wilson JG, Harris CR, Jeffrey DW (1980) Problems in the assessment of heavy-metal levels in estuaries and the formation of a pollution index. Helgoland Mar. Res 33:566–575
49. Appleby PG (2001) Chronostratigraphic techniques in recent sediments. In: Last WM, Smol JP (eds) Tracking environmental change using lake sediments. volume 1: basin analysis, coring, and chronological techniques, vol 1. Kluwer, Dordrecht, pp 171–203
50. Van Geen A, Valette-Silver NJ, Luoma SN, Fuller CC, Baskaran M, Tera F, Klein J (1999) Constraints on the sedimentation history of San Francisco Bay from ^{14}C and ^{10}Be. Mar Chem 64:29–38
51. Gomes FC, Godoy JM, Godoy MLDP, Carvalho ZL, Lopes RT, Sanchez-Cabeza JA, Osvath I, Lacerda LD (2011) Geochronology of anthropogenic radionuclides in Ribeira Bay sediments, Rio de Janeiro, Brasil. J Environ Radioact 102(9):871–876
52. Karageorgis AP, Kaberi H, Price NB, Muir GKP, Pates JM, Lykousis V (2005) Chemical composition of short sediment cores from Thermaikos Gulf (Eastern Mediteranean): sediment accumulation rates, trawling and winnowing effects. Cont Shelf Res 25:2456–2475
53. Baskaran M (2011) Po-210 and Pb-210 as atmospheric tracers and global atmospheric Pb-210 fallout: a review. J Environ Radioact 102:500–513
54. Garcia-Orellana J, Sanchez-Cabeza JA, Masque P, Àvilla A, Costa E, Loÿe-Pilot MD, Bruach-Menchén JM (2006) Atmospheric fluxes of 210Pb to the western Mediterranean Sea and Saharan dust influence. J Geophys Res 111(D15305):1–9
55. Krishnaswami S, Lal D (1978) Radionuclide limnochronology. ss 153–177. Lerman A ed. Lakes-chemistry geology physics. 1978. Springer, New York
56. O'Reilly J, Vintró LL, Mitchell PI, Donohue I, Leira M, Hobbs W, Irvine K (2011) 210Pb-dating of a lake sediment core from Lough Carra (Co. Mayo, western Ireland): use of paleolimnological data for chronology validation below the 210Pb dating horizon. J Environ Radioact 102:495–499
57. Farmer JG, Eades LJ, MacKenzie AB, Kirika A, Bailey-Watts TE (1996) Stable lead isotope record of lead pollution in Loch Lomond sediments since 163 A.D. Environ Sci Technol 30:3080–3083
58. Komárek M, Ettler V, Chrastný V, Mihaljevič M (2008) Led isotopes in environmental sciences: a review. Environ Int 34:562–577